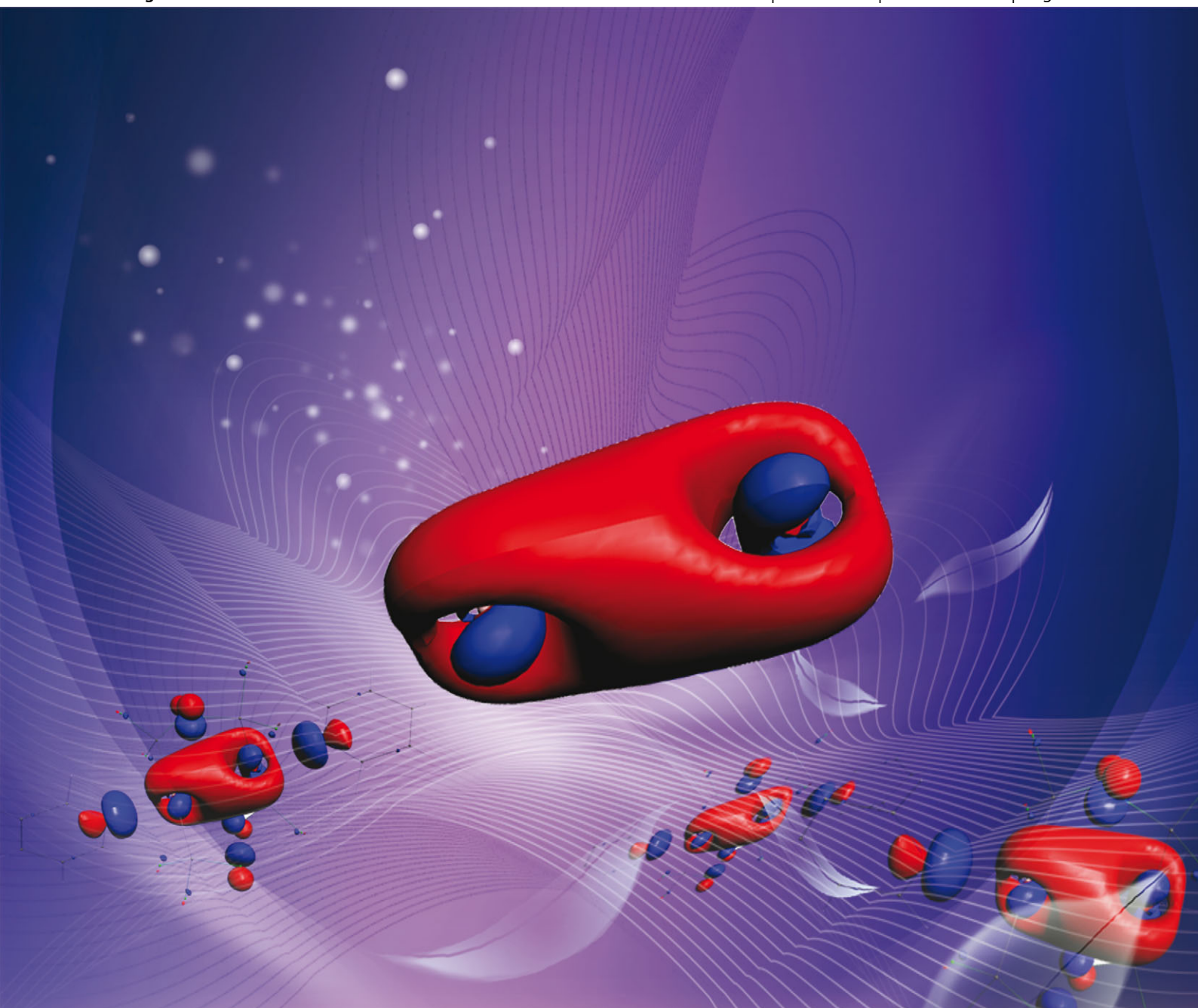


# ChemComm

Chemical Communications

[www.rsc.org/chemcomm](http://www.rsc.org/chemcomm)

Volume 49 | Number 21 | 14 March 2013 | Pages 2073–2162



ISSN 1359-7345

RSC Publishing

**COMMUNICATION**

Xiao-Gen Xiong and Pekka Pyykkö  
Unbridged Au(II)–Au(II) bonds are theoretically allowed



1359-7345(2013)49:21;1-9

# Unbridged Au(II)–Au(II) bonds are theoretically allowed†

Xiao-Gen Xiong<sup>ab</sup> and Pekka Pyykkö<sup>\*b</sup>

Cite this: *Chem. Commun.*, 2013, **49**, 2103

Received 30th October 2012,  
Accepted 3rd January 2013

DOI: 10.1039/c2cc37875b

www.rsc.org/chemcomm

**The bonding in the unbridged closed-shell Au(II)–Au(II) dimers  $X_4Au_2(C_5H_5N)_2$ ,  $X = H, F-I$  and  $CF_3$ , is analyzed and the short Au–Au bonds around 250 pm are reproduced by a novel  $6s6p_25d_{xy}$  hybridization.**

Short Au(II)–Au(II) bonds of 269.7(1)–297.7(10) pm are experimentally known in systems like  $[Au_2(i-MNT)_2]^{2-}$  (*i*-MNT:1,1-dicyanoethene-2,2-dithiolate).<sup>1</sup> Common to all of them is that the two ligand atoms are coupled by a bridge. The bonding in these systems has been analyzed using semiempirical methods by Hoffmann's group<sup>2</sup> and later, using *ab initio* methods, by us.<sup>3</sup> Recently two cases with unbridged Au(II)–Au(II) bonds were reported.<sup>4,5</sup> Earlier examples were reported by the groups of Yam<sup>6,7</sup> and Raubenheimer.<sup>8</sup> Common to all these cases were nearly perpendicular Au (CN = 4) planes and short Au(II)–Au(II) bonds of the order of 249–264 pm. We here account for both observations by performing a DFT study on the model systems  $X_4Au_2(C_5H_5N)_2$ ,  $X = H, F-I$  and  $CF_3$ . It should be noted that, in contrast to the ubiquitous Au(I)–Au(I) closed-shell "aurophilic" attractions which are basically of dispersion type,<sup>1</sup> we here expect a dominant covalent bond.

The optimized PBE geometries of the model systems<sup>9</sup> are listed in Table 1. All of them have a very short unsupported

**Table 1** Optimized geometries of  $X_4Au_2(C_5H_5N)_2$ ,  $X = H, F-I$  and  $CF_3$ , all bond lengths in pm and all angles in degrees

X	$R(Au-Au)$	$R(Au-N)$	$R(Au-X)$	$\angle XAuX$	$\angle XAuN$
H	250.7	217.0	165.4	173.5	93.3
F	254.4	218.1	196.9	179.0	89.5
Cl	256.6	220.4	231.9	174.7	92.7
Br	256.5	219.0	248.3	174.0	93.0
I	257.4	219.0	267.0	173.0	93.5
$CF_3$	255.3	217.5	212.2	178.2	89.1

<sup>a</sup> Department of Chemistry, Tsinghua University, 100 084 Beijing, China

<sup>b</sup> Department of Chemistry, University of Helsinki, P.O.B. 55, FI-00014 Helsinki, Finland. E-mail: Pekka.Pyykkö@helsinki.fi; Fax: +358 9 191 50169; Tel: +358 9 191 50171

† Electronic supplementary information (ESI) available. See DOI: 10.1039/c2cc37875b

Au(II)–Au(II) bond. One thing that should be noted is that, in all cases, the N–Au–Au–N backbones are linear. All molecules except  $(CF_3)_4Au_2(C_5H_5N)_2$  are confirmed to possess  $D_2$  symmetry, while the latter one has  $C_2$  symmetry. The  $R(Au-Au)$  of  $(CF_3)_4Au_2(C_5H_5N)_2$  in our calculation is 255.3 pm, while one experimental value is 250.62(9) pm.<sup>4</sup> Note the position of  $-CF_3$  between F and Cl, coherent with the electronegativity data of García *et al.*<sup>10</sup> Further calculations with hybrid, meta-GGA and hybrid meta-GGA functionals were also carried out; the geometries are listed in the ESI† and the results also confirm the existence of a short, unsupported Au(II)–Au(II) bond.

In order to investigate the Au(II)–Au(II) bond, we carried out a population analysis and calculated bond orders using a variety of theoretical approaches.<sup>11–18</sup> The calculated atomic charges and bond orders are given in Tables 2 and 3. All methods show

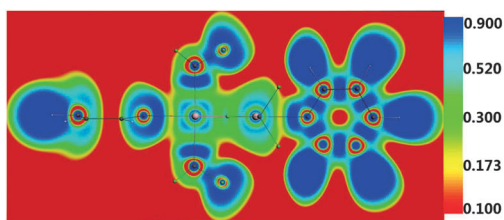
**Table 2** Atomic charges of  $X_4Au_2(C_5H_5N)_2$ ,  $X = H, F-I$  and  $CF_3$ , calculated with Hirshfeld,<sup>11</sup> Voronoi,<sup>12</sup> MDC-q<sup>13</sup> (Multipole-Derived Charge densities), and AIM<sup>14,15</sup> (Atoms in Molecules) formalisms

X	Atom	Hirshfeld	Voronoi	MDC-q	AIM
H	Au	0.12	0.29	0.56	0.25
	H	−0.17	−0.26	−0.37	−0.22
	N	−0.06	−0.07	0.42	−0.96
F	Au	0.37	0.36	0.74	0.92
	F	−0.31	−0.32	−0.52	−0.60
	N	−0.06	−0.06	−0.32	−0.97
Cl	Au	0.29	0.31	0.35	0.59
	Cl	−0.25	−0.28	−0.33	−0.42
	N	−0.06	−0.07	0.01	−0.95
Br	Au	0.25	0.26	0.43	0.45
	Br	−0.23	−0.26	−0.37	−0.34
	N	−0.06	−0.07	0.19	−1.01
I	Au	0.20	0.19	0.27	0.26
	I	−0.21	−0.22	−0.28	−0.25
	N	−0.07	−0.07	0.33	−1.02
$CF_3$	Au	0.25	0.25	0.41	0.48
	C	0.10	0.08	−0.09	1.44
	N	−0.06	−0.08	−0.34	−1.00



**Table 3** Bond orders of  $X_4Au_2(C_5H_5N)_2$ , X = H, F-I and  $CF_3$ , calculated with Mayer,<sup>16</sup> G-J (Gopinathan-Jug)<sup>17</sup> and N-M (Nalewajski-Mrozek)<sup>18</sup> formalisms

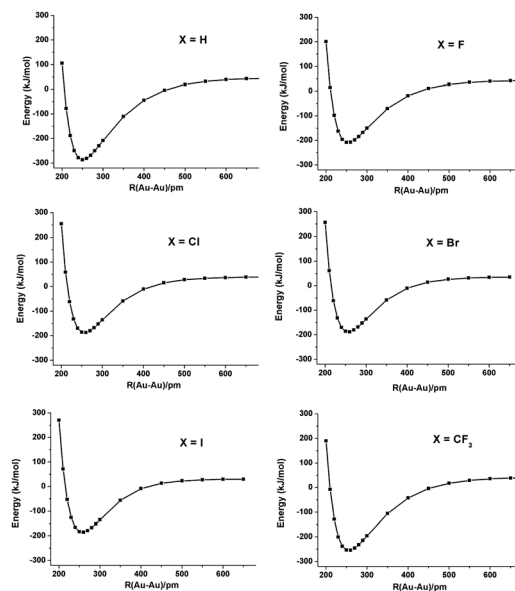
X	Bond	Mayer	G-J	N-M(3)
H	Au-Au	0.77	0.46	0.27
	Au-N	0.40	0.24	0.21
	Au-H	0.76	0.43	0.46
F	Au-Au	0.74	0.43	0.22
	Au-N	0.38	0.24	0.20
	Au-F	0.59	0.47	0.74
Cl	Au-Au	0.67	0.38	0.20
	Au-N	0.40	0.25	0.21
	Au-Cl	0.78	0.49	0.65
Br	Au-Au	0.66	0.38	0.20
	Au-N	0.41	0.25	0.21
	Au-Br	0.67	0.47	0.61
I	Au-Au	0.65	0.36	0.21
	Au-N	0.42	0.25	0.22
	Au-I	0.79	0.46	0.56
$CF_3$	Au-Au	0.83	0.42	0.22
	Au-N	0.44	0.14	0.19
	Au-C	0.74	0.45	0.33

**Fig. 1** The electron localization functions (ELFs) of  $(CF_3)_4Au_2(C_5H_5N)_2$ . From left, the atoms are N-Au-Au-N.

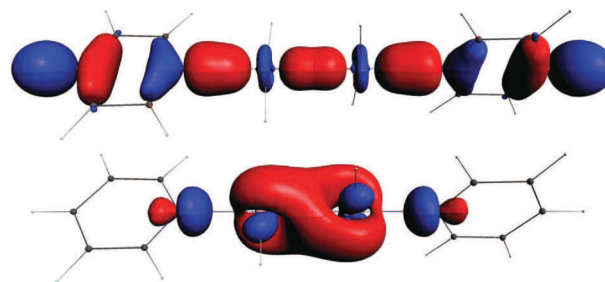
that the two Au atoms are positively charged. The calculated electron localization functions (ELFs, in Fig. 1) show that there is clearly electron pair density between the two Au atoms. The Au(II)-Au(II) bonding energy curves are shown in Fig. 2. Here the bonding energy is defined as the energy difference between the complex and two  $X_2Au(C_5H_5N)$  monomers. The geometries of two monomers are fixed to the optimized  $X_4Au_2(C_5H_5N)_2$  geometry and only the distance of two Au atoms is varied. The Au-Au bonding energy is approximately  $200 \text{ kJ mol}^{-1}$ , and varied with the ligands. The bonding energies at the equilibrium geometry are listed in Table 4.

The Kohn-Sham bonding orbitals for the Au-Au bonds are of the, perhaps less obvious, types given in Fig. 3. Here the X = H is selected. The experimental case X =  $-CF_3$  is shown in the graphical abstract. Both cases show an spd or more precisely  $6s5d_{xy}6p_z$  hybridization. The percentages for X =  $-CF_3$  are 6s 31%, 5d 12%, 6p<sub>z</sub> 10%. We have not previously seen a hybridization like this.<sup>19-21</sup>

In order to probe the stabilizing effect of the axial ligand, two other ligands,  $-CH_3$  and  $NH_3$ , were chosen to replace pyridine. The unbridged Au(II)-Au(II) bond also exists when pyridine is replaced by  $NH_3$ , but  $-CH_3$ , leading to Au(III), will destabilize the Au-Au bond, see the ESI.†

**Fig. 2** Au(II)-Au(II) bonding energy curves of  $X_4Au_2(C_5H_5N)_2$ , X = H, F-I and  $CF_3$ . The geometry of  $X_2Au(C_5H_5N)$  was fixed to the monomer geometry in the complex.**Table 4** Bonding energies of  $X_4Au_2(C_5H_5N)_2$  (X = H, F-I and  $CF_3$ ) at the equilibrium geometry, all energies are in  $\text{kJ mol}^{-1}$ 

X	H	F	Cl	Br	I	$CF_3$
Bonding energy	286.3	209.1	188.1	188.5	185.7	255.2

**Fig. 3** The Au(II)-Au(II) bonding orbitals of  $H_4Au_2(C_5H_5N)_2$  (isosurf. = 0.05 a.u.). For the real-world case X =  $-CF_3$ , see the graphical abstract.

In conclusion, using DFT calculations, we investigated the unsupported Au(II)-Au(II) bond in the model system  $X_4Au_2(C_5H_5N)_2$ , X = H, F-I and  $CF_3$ . The bond length of Au-Au is located in the covalent Au-Au region. All the theoretical results clearly show the covalent nature of the unsupported Au(II)-Au(II) bond in these molecules.

Computational methods: all calculations were performed with density functional theory (DFT). Generalized gradient approximation (GGA) with the PBE exchange-correlation functional<sup>9</sup> implemented in the Amsterdam Density Functional program (ADF 2010.01)<sup>22</sup> was used. The Slater basis sets with the quality of triple- $\zeta$  plus two polarization functions (TZ2P) with the frozen-core approximation applied to inner shells were used. The scalar-relativistic (SR) effects were taken into account



by the zero-order-regular approximation (ZORA).<sup>23</sup> Geometries were fully optimized at the SR-ZORA level. Vibrational frequency calculations were also carried out at the SR-ZORA level with the PBE functional to confirm the minima. In order to confirm our results, we performed further DFT calculations with hybrid, meta-GGA and hybrid meta-GGA functionals, implemented in Gaussian09.<sup>24</sup> The computational details of Gaussian calculations can be found in the ESI.† Spin-orbit effects were tested at the ZORA level in the X = H case and found negligible.

The work of XGX at Helsinki is supported by the China Scholarship Council. Computer resources were obtained from the Centre for Scientific Computing, Finland.

## References

- 1 P. Pyykkö, *Chem. Rev.*, 1997, **97**, 597–636.
- 2 Y. Jiang, S. Alvarez and R. Hoffmann, *Inorg. Chem.*, 1985, **24**, 749–757.
- 3 P. Pyykkö and F. Mendizabal, *Inorg. Chem.*, 1998, **37**, 3018–3025.
- 4 D. Zopes, C. Hegemann, W. Tyrre and S. Mathur, *Chem. Commun.*, 2012, **48**, 8805–8807.
- 5 D.-A. Roşca, D. A. Smith, D. L. Hughes and M. Bochmann, *Angew. Chem., Int. Ed.*, 2012, **51**, 10643–10646.
- 6 V. W.-W. Yam, S. W.-K. Choi and K.-K. Cheung, *Chem. Commun.*, 1996, 1173–1174.
- 7 V. W.-W. Yam, C.-K. Li, C.-L. Chan and K.-K. Cheung, *Inorg. Chem.*, 2001, **40**, 7054–7058.
- 8 J. Coetzee, W. F. Gabrielli, K. Coetzee, O. Schuster, S. D. Nogai, S. Cronje and H. G. Raubenheimer, *Angew. Chem., Int. Ed.*, 2007, **46**, 2497–2500.
- 9 J. P. Perdew, K. Burke and M. Ernzerhof, *Phys. Rev. Lett.*, 1996, **77**, 3865–3868.
- 10 A. García-Monforte, S. Martínez-Salvador and B. Menjón, *Eur. J. Inorg. Chem.*, 2012, 4945–4966.
- 11 F. L. Hirshfeld, *Theor. Chem. Acc.*, 1977, **44**, 129–138.
- 12 F. M. Bickelhaupt, N. J. R. van Eikema Hommes, C. Fonseca Guerra and E. J. Baerends, *Organometallics*, 1996, **15**, 2923–2931.
- 13 M. Swart, P. T. van Duijnen and J. G. Snijders, *J. Comput. Chem.*, 2001, **22**, 79–88.
- 14 J. I. Rodríguez, R. F. Bader, P. W. Ayers, C. Michel, A. W. Götz and C. Bo, *Chem. Phys. Lett.*, 2009, **472**, 149–152.
- 15 J. I. Rodríguez, A. M. Köster, P. W. Ayers, A. Santos-Valle, A. Vela and G. Merino, *J. Comput. Chem.*, 2009, **30**, 1082–1092.
- 16 I. Mayer, *Chem. Phys. Lett.*, 1983, **97**, 270–274.
- 17 M. S. Gopinathan and K. Jug, *Theor. Chem. Acc.*, 1983, **63**, 497–509.
- 18 A. Michalak, R. L. DeKock and T. Ziegler, *J. Phys. Chem. A*, 2008, **112**, 7256–7263.
- 19 Note that the bonding orbital in Fig. 3b has no conspicuous nodes in the Au–Au part while a  $d_{xy}$ – $d_{xy}$  bond would have two. Such a “screw, don’t split” principle is not unlike the “angular nodes” explanation for the 18e principle.
- 20 P. Pyykkö, *J. Organomet. Chem.*, 2006, **691**, 4336–4340.
- 21 The  $d_{xy}$  on atom A bonds here to the  $d_{x^2-y^2}$  on atom B.
- 22 <http://www.scm.com>.
- 23 E. van Lenthe, R. van Leeuwen, E. J. Baerends and J. G. Snijders, *Int. J. Quantum Chem.*, 1996, **57**, 281–293.
- 24 M. J. Frisch, G. W. Trucks, H. B. Schlegel, G. E. Scuseria, M. A. Robb, J. R. Cheeseman, G. Scalmani, V. Barone, B. Mennucci, G. A. Petersson, H. Nakatsuji, M. Caricato, X. Li, H. P. Hratchian, A. F. Izmaylov, J. Bloino, G. Zheng, J. L. Sonnenberg, M. Hada, M. Ehara, K. Toyota, R. Fukuda, J. Hasegawa, M. Ishida, T. Nakajima, Y. Honda, O. Kitao, H. Nakai, T. Vreven, J. A. Montgomery Jr., J. E. Peralta, F. Ogliaro, M. Bearpark, J. J. Heyd, E. Brothers, K. N. Kudin, V. N. Staroverov, R. Kobayashi, J. Normand, K. Raghavachari, A. Rendell, J. C. Burant, S. S. Iyengar, J. Tomasi, M. Cossi, N. Rega, J. M. Millam, M. Klene, J. E. Knox, J. B. Cross, V. Bakken, C. Adamo, J. Jaramillo, R. Gomperts, R. E. Stratmann, O. Yazyev, A. J. Austin, R. Cammi, C. Pomelli, J. W. Ochterski, R. L. Martin, K. Morokuma, V. G. Zakrzewski, G. A. Voth, P. Salvador, J. J. Dannenberg, S. Dapprich, A. D. Daniels, O. Farkas, J. B. Foresman, J. V. Ortiz, J. Cioslowski and D. J. Fox, *Gaussian 09 Revision A.1*, Gaussian Inc., Wallingford, CT, 2009.

